Modeling Earth Systems and Environment (2025) 11:230
https://doi.org/10.1007/s40808-025-02398-9

ORIGINAL ARTICLE

Exploring the fixed point theory and numerical modeling of fish harvesting system with Allee effect

Muhammad Waqas Yasin[1] · Mobeen Akhtar[1] · Nauman Ahmed[2] · Ali Akgül[3,4,5,6] · Qasem Al-Mdallal[7]

Received: 20 February 2025 / Accepted: 25 March 2025

Abstract
Fish harvesting has a major role in nutritive food that is easily accessible for human nourishment. In this article, a reaction-diffusion fish harvesting model with the Allee effect is analyzed. The study of population models is a need of this hour because by using precautionary measures, mankind can handle the issue of food better. The basic mathematical properties are studied such as equilibrium analysis, stability, and consistency of this model. The Implicit finite difference and backward Euler methods are used for the computational results of the underlying model. The linear analysis of both schemes is derived and schemes are unconditionally stable. By using the Taylor series consistency of both schemes is proved. The positivity of the Implicit finite difference scheme is proved by using the induction technique. A test problem has been used for the numerical results. For the various values of the parameters, the simulations are drawn. The dynamical properties of continuous models, like positivity, are absent from the simulations produced by the backward Euler scheme. Implicit finite difference scheme preserves the dynamical properties of the model such as positivity, consistency, and stability. Simulations of the test problem prove the effectiveness of the Implicit finite difference scheme.

Keywords Reaction-diffusion model · Allee effect · Holling type II · Implicit finite difference scheme · Backward Euler scheme · Analysis · Simulations

Introduction

Fish harvesting models are used in real-world fisheries management to forecast the effects of fishing practices on fish stocks, guide sustainable harvesting practices, and guarantee the long-term health of fish populations. These models simulate fish population dynamics and harvesting effects using mathematical equations. If we consider variables such as fishing effort, fertility rates, and mortality rate, these models assist in forecasting how fish populations will fluctuate over time under various harvesting strategies. There are some real-world applications of the fish harvesting model such as these models are used by the National Oceanic and Atmospheric Administration to manage American fisheries, including those in the Pacific region and West of Mexico and other countries as well. These models are used by agencies such as the United Nations Food and Agriculture Organization to promote sustainable fisheries management across the globe while scientists also refine the fish harvesting models for accuracy and predictive power. The accuracy of this model is determined by the quality and accessibility of data on fish populations, fishing efforts, and environmental conditions.

✉ Ali Akgül
aliakgul00727@gmail.com

Nauman Ahmed
nauman.ahmd01@gmail.com

[1] Department of mathematics, University of Narowal, Narowal, Pakistan

[2] Department of Mathematics and Statistics, The University of Lahore, Lahore, Pakistan

[3] Department of Electronics and Communication Engineering, Saveetha School of Engineering, SIMATS, Chennai, Tamilnadu, India

[4] Department of Mathematics, Art and Science Faculty, Siirt University, 56100 Siirt, Turkey

[5] Department of Mathematics, Mathematics Research Center, Near East University, Near East Boulevard, 99138 Nicosia/Mersin 10, Turkey

[6] Department of Computer Engineering, Biruni University, 34010 Topkapi, Istanbul, Turkey

[7] Department of Mathematical Sciences, UAE University, P.O. Box 17551, Al Ain, United Arab Emirates

Published online: 24 April 2025

Since there are always some uncertainties in these models, managers must be conscious of their limitations and base their decisions on a combination of information and model predictions.

Fishing, which dates back to 40.000 BC, is one of the oldest human activities. Fish are a significant food source, but they are also profitable and used to make a variety of items that are not intended for human consumption. One of the best cost-effective investments right now is fishing. When fishing from natural resources, the fishing cost depends on the apparatus and labor required to operate them, with no expenditures associated with fish production. With the Industrial Revolution, fishing methods and artificial fish production techniques both advanced significantly. Differential equations are used to express the complicated natural phenomena in mathematical language by using a set of equations (Younas et al. 2022; Ahmed et al. 2023a, b; Ali et al. 2023; Younis et al. 2021; Seadawy et al. 2022)

In the literature, there is a variety of models in this field that put out and explain the fish population under harvesting activity. Cushing and Saleem discussed a prey-predator model where the population of predators shows the structure of age which significantly affects its fertility. They derived basic McKendrick equations, for an age-designed population (Cushing and Saleem 1982). Cooke and Nusse investigated discrete single-species population models with harvesting in a qualitative manner (Cooke and Nusse 1987). Idels and Wang formulate a fish model that trusts on the density consequence of fish population and is based on the canonical differential equation model (Idels and Wang 2008). González-Olivares et al. examined a model i.e. prey-predator and its overall behavior with Gause type in consideration of dual features which are prey evaluation that is affected by Allee effects and secondly functional outputs in Holling type III (González-Olivares et al. 2011). González-Olivares and Rojas-Palma examine the most popular calculated results to depict the Allee effects on prey growth that are taken into consideration of the prey-predator model and built after the Gower Leslie form model (González-Olivares and Rojas-Palma 2011).

Rojas-Palma and González-Olivares focused on determining the best harvesting strategy, in an open-access fishery with non-selective harvesting together predator–prey species (Rojas-Palma and González-Olivares 2012). González-Olivares and Rojas-Palma structural stability of predator–prey models having Gause type examined in this context of three conventional practical reactions and an Allee effect on the development rate of prey (González-Olivares and Rojas-Palma 2013). Daci and Spaho studied some of the various bifurcations that can occur in some dynamical systems in one dimension and also discussed how these bifurcations can be used to study population dynamics, particularly in aquaculture (Daci and Spaho 2013). Perälä and Kuparinen studied Bayesian statistical methods to analyze nine populations and solve a challenge about the widely held belief that allee effects are rare. They evaluated a result about the population that, when Allee effects are present or compensation, the same species shows strong evidence (Perälä and Kuparinen 2017). Alfred examined the harvesting techniques used in wrasse fish farming, the logistic development of models is: proportional, constant, and periodical harvesting. The ideal quantity of fish to be taken for each approach is assessed to prevent the population from going extinct (Alfred 2016).

Saber et al. by adding a time delay to the associated term between insulin and glucose, this study expands previous research. The stability properties of the new model have been assessed. The outcomes of the theory are validated using simulations with numerical values (Saber et al. 2018). Selvam et al. considered the Allee effect along with the Holling-type reaction function in the prey-predator model. Distinct two-species systems of fractional order exist. In comparison to its corresponding continuous version, also dynamics of the discretized system are considerably more complex and rich (Selvam et al. 2018). González-Olivares et al. discussed a well-known model that is modified Volterra model along with incorporated descriptions. A straightforward and potent Allee effect impacting the population of prey animals will also be taken into account in the context of this ecological occurrence (González-Olivares et al. 2019). Dunn and Hovel used the way a consumer responds to a change in resource density as a reliable and common approach for estimating the significance of consumption to the stability and dynamics of populations (Dunn and Hovel 2020). Brites and Braumann used stochastic DE when there was a weak Allee effect and modeled the dynamics of the harvested population. Two optimum harvesting strategies are offered, one of which is optimal control theory for practical uses and inappropriate in an arbitrary situation (Brites and Braumann 2020).

Tesfay et al. studied the stochastic growth model in the presence or absence of the Allee effect. They analyzed the extinction probability of the population using the Fokker–Planck equation. Further studied the impact of harvesting rate, Allee effect, and noise intensity on population evaluation (Tesfay et al. 2021). Huang et al. discussed the best fishing practices for both marine protected areas and open waters. The fish population is considered to grow by a specific growth law throughout the literature (Huang et al. 2020). Diz-Pita and Otero-Espinar reviewed some interesting properties of the prey-predator model and gave a recent state-of-the-art review of these characteristics which are the fear effect, Allee effects, immigration, and cannibalism (Diz-Pita and Otero-Espinar 2021). Bashier et al. provided a differential equations model that explains how fish population dynamics change when fishing activity

is present. When there are no harvesting operations, they assume that logistic growth with the Allee effect governs the population of fish dynamics expansion (Bashier 2023). The main idea of this article is to form a system of Fish Farm having spatial diffusion and give numerical solutions. They considered the Fish harvesting model with Allee effects. The authors used Burgers' equation is numerically solved using B-spline collocation with Euler (Gupta and Kadalbajoo 2016). Gupta et al. (2021) constructed a finite difference scheme for a class of interior turning point problems that are singularly perturbed. Some other authors developed and analyzed a finite difference method for convection-diffusion problems with time-fractional singular perturbations (Sahoo and Gupta 2023). Using a numerical scheme, other researchers examined a singularly perturbed convection-diffusion problem with discontinuous convective and supply terms (Sahoo and Gupta 2022). The authors proposed technique for the stability analysis of discrete-time systems (Guo et al. 2021), stability of Boolean networks (Guo et al. 2015), finite-time control strategy to solve the motion control problem (Lv et al. 2022), and some more work is given in Wu et al. (2021), Shi et al. (2024).

In Bashier (2023), the authors considered the fish harvesting model with the Allee effect as given below

$$\frac{dN}{dt} = rN(t)\left(\frac{N(t)}{M} - 1\right)\left(1 - \frac{N(t)}{k}\right) - \frac{pqN(t)E(t)}{k + N(t)}, \tag{1}$$

$$\frac{dE}{dt} = \alpha\left(\frac{pqN(t)E(t)}{k + N(t)} - cE(t)\right). \tag{2}$$

With given initial and homogeneous Neumann boundary conditions.

$$N(0) = N_0 \tag{3}$$

$$E(0) = E_0. \tag{4}$$

The authors proposed a system of two ordinary differential equations (Bashier 2023) representing the harvesting of fishes, where the dynamics of the fish population is represented by a logistic model with Alee effect, and the second equation describes the dynamics of the harvesting effort exerted to catch the fishes. As fish population can move from one place to another. The spatial movement of the fish population can not be ignored. So, we considered the fish population model under the effect of diffusion phenomena and its impact on the model is numerically analyzed. If the parameter M is close to zero then it is a weak Allee effect and if M is significantly greater than zero then it is a strong Allee effect.

The fish farm model under the effect of diffusion phenomena is given as

$$\frac{\partial N}{\partial t} = d_N N_{xx} + rN(x,t)\left(\frac{N(x,t)}{M} - 1\right)\left(1 - \frac{N(x,t)}{K}\right) - \frac{pqN(x,t)E(x,t)}{k + N(x,t)}, \tag{5}$$

$$\frac{\partial E}{\partial t} = d_E E_{xx} + \alpha\left(\frac{pqN(x,t)E(x,t)}{k + N(x,t)} - cE(x,t)\right). \tag{6}$$

corresponding initial conditions are,

$$N(x,0) = N_0(x) \tag{7}$$

$$E(x,0) = E_0(x). \tag{8}$$

The $N(x, t)$ and $E(x, t)$ represent the dynamics of the fish population and the effort used to catch them. There are two compartments of the models, one is that contain the population of the fishes and the second is the effort applied to the catchment of them. The d_N, d_E are the diffusion coefficients, p, c, and α are the average unit price, per unit cost, and catchability parameter respectively. The $\frac{pqN(x,t)E(x,t)}{k+N(x,t)}$ is the functional response.

Being a population model, the solutions of the underlying model are obtained by ordinary methods and may contain negative behavior which is biologically not possible, it is also possible to have unbounded behavior for a given system. Therefore, the an urgent need to consider a scheme that preserves essential properties of a continuous system. Regarding this, we have used two schemes, one is the backward Euler scheme, and its results are bounded and have negative behavior as well that is not suitable for the continuous system. On the other hand, an Implicit finite difference scheme is used. Its positivity is proved by using M-matrices and induction theory. Numerical results obtained by this scheme are convergent, bounded, stable, and positive behavior. It contains all the necessary properties of a continuous system. So, such a scheme has an advantage over the other scheme due to its efficient results. The fact that there is a special solution analyzed in the upcoming section.

Unique existence

This section is devoted to establishing the unique existence of the system (5–6). To show that solutions exist, we can use a technique called the fixed-point theorem. This theorem helps us find solutions that match the initial conditions and how things are at the edges of our area of study. Making sure there's only one solution (uniqueness) is also super important because it helps us be confident in the model's predictions. We use other methods, like the contraction mapping principle, to prove uniqueness (Iqbal 2011). By

using these math tools, we can better understand the model and how it can help us manage fisheries and protect fish populations. For this sake, we integrate the system (5–6) and we have the following fixed point operator

$$\mathrm{T}_N(x,t) = N_0(x) + \int_0^t \left(d_N N_{xx} + rN(x,\xi)\left(\frac{N(x,\xi)}{M} - 1\right) \times \left(1 - \frac{N(x,\xi)}{K}\right) - \frac{qN(x,\xi)E(x,\xi)}{k + N(x,\xi)} \right) d\xi, \tag{9}$$

$$\mathrm{T}_E(x,t) = E_0(x) + \int_0^t \left(d_E E_{xx} + \alpha\left(\frac{pqN(x,\xi)E(x,\xi)}{k + N(x,\xi)} - cE(x,\xi)\right)\right) d\xi, \tag{10}$$

now we assume two closed ball B_N and B_E in the space C of all solution functions such that

$$B_N = B_{r^*}(N_0) = \{N, N \in C[0,L] : ||N - N_0|| \le r^*\}, \quad ||N|| \le (r^* + N_0) \quad \because N_0 > 0, \tag{11}$$

$$B_E = B_{r^*}(E_0) = \{E, E \in C[0,L] : ||E - E_0|| \le r^*\}, \quad ||E|| \le (r^* + E_0) \quad \because E_0 > 0. \tag{12}$$

where N_0 and E_0 are centers and r^* is the radius. These closed balls are optimal closed bounded and convex subsets of the space C and we show that a unique solution to then each equation lies in these subsets. For this purpose, we evaluate a couple of conditions for each fixed point operator namely the self and contraction mappings (Iqbal et al. 2022).

Self mapping

Consider the operator (9) and taking norm on both sides such that

$$||\mathrm{T}_N(x,t) - N_0(x)|| \le \int_0^t \left(|d_N|||N_{xx}|| + |r|||N||\left(\frac{||N||}{|M|} + 1\right) \times \left(1 + \frac{||N||}{|K|}\right) + \frac{|q|||N||||E||}{|k| + ||N||}\right) d\xi,$$

now applying embedding theorem (Shahzad et al. 2023) of compact spaces we have

$$||N_{xx}|| \le \kappa_1 ||N||$$

so that

$$||\mathrm{T}_N(x,t) - N_0(x)|| \le \int_0^t \left(|d_N|\kappa_1||N|| + |r|||N||\left(\frac{||N||}{|M|} + 1\right) \left(1 + \frac{||N||}{|K|}\right) + \frac{|q|||N||||E||}{|k| + ||N||}\right) d\xi,$$

now from (11–12) we get

$$||\mathrm{T}_N(x,t) - N_0(x)|| \le \int_0^t \left(|d_N|\kappa_1(r + N_0) + |r|(r + N_0)\left(\frac{(r^* + N_0)}{|M|} + 1\right) \times \left(1 + \frac{(r^* + N_0)}{|K|}\right) + \frac{|q|(r^* + N_0)(r^* + E_0)}{|k| + (r^* + N_0)}\right) d\xi,$$

put the constant

$$b = \max\{N_0, E_0\}$$

such that

$$||\mathrm{T}_N(x,t) - N_0(x)|| \le \int_0^t \left(|d_N|\kappa_1(r + b) + |r|(r^* + b)\left(\frac{(r^* + b)}{|M|} + 1\right) \times \left(1 + \frac{(r^* + b)}{|K|}\right) + \frac{|q|(r^* + b)(r^* + b)}{|k| + (r^* + b)}\right) d\xi,$$

now

$$||\mathrm{T}_N(x,t) - N_0(x)|| \le \left(|d_N|\kappa_1(b + r^*) + |r|(b + r^*)\left(\frac{(b + r^*)}{|M|} + 1\right)\left(1 + \frac{(b + r^*)}{|K|}\right) + \frac{|q|(b + r^*)(b + r^*)}{|k| + (b + r^*)}\right) \int_0^t d\xi,$$

and

$$||\mathrm{T}_N(x,t) - N_0(x)|| \le \left(|d_N|\kappa_1(b + r^*) + |r|(b + r^*)\left(\frac{(b + r^*)}{|M|} + 1\right)\left(1 + \frac{(b + r^*)}{|K|}\right) + \frac{|q|(b + r^*)(b + r^*)}{|k| + (b + r^*)}\right) L,$$

for each self-mapping in any closed ball, we know that the distance from the function point to a center is always less are equal to the radius such that

$$||\mathrm{T}_N(x,t) - N_0(x)|| \le r$$

therefore

$$\left(|d_N|\kappa_1(b + r^*) + |r|(b + r^*)\left(\frac{(b + r^*)}{|M|} + 1\right)\left(1 + \frac{(b + r^*)}{|K|}\right) + \frac{|q|(b + r^*)(b + r^*)}{|k| + (b + r^*)}\right) L \le r,$$

hence

$$L \le \frac{r}{\left(|d_N|\kappa_1(b + r^*) + |r|(b + r^*)\left(\frac{(b + r^*)}{|M|} + 1\right)\left(1 + \frac{(b + r^*)}{|K|}\right) + \frac{|q|(b + r^*)(b + r^*)}{|k| + (b + r^*)}\right)},$$

or

$$L_{N^s} \le \frac{r}{\left(|d_N|\kappa_1(b + r^*) + |r|(b + r^*)\left(\frac{(b + r^*)}{|M|} + 1\right)\left(1 + \frac{(b + r^*)}{|K|}\right) + \frac{|q|(b + r^*)(b + r^*)}{|k| + (b + r^*)}\right)},$$

which is the condition of self-mapping for the operator (9). and similarly, we find the condition of self-mapping for the operator (10) such that

$$L_{E^s} \leq \frac{r}{\left(\left(d_E\kappa_2(b+r^*)+\alpha\left(\frac{pq(b+r^*)^2}{k+(b+r^*)}+c(b+r^*)\right)\right)\right)},$$

Lemma 1 Under the conditions of L_{N^s} and L_{E^s} the fixed point operators (5)–(6) have at least one fixed point in the closed and convex subsets B_N and B_E of space $C[0, \frac{r}{\left(|d_N|\kappa_1(r^*+b)+|r|(r^*+b)\left(\frac{(r^*+b)}{|M|}+1\right)\left(1+\frac{(r^*+b)}{|K|}\right)+\frac{|q|(r^*+b)(r^*+b)}{|k|+(r^*+b)}\right)}]$ and $C[0, \frac{r}{\left(\left(d_E\kappa_2(r^*+b)+\alpha\left(\frac{pq(r^*+b)^2}{k+(r^*+b)}+c(r^*+b)\right)\right)\right)}]$.

Contraction mapping

Consider the operator (9)

$$\mathrm{T}_N(x,t) = N_0(x) + \int_0^t \left(d_N N_{xx} + rN(x,\xi)\left(\frac{N(x,\xi)}{M}-1\right) \times \left(1-\frac{N(x,\xi)}{K}\right) - \frac{qN(x,\xi)E(x,\xi)}{k+N(x,\xi)}\right)d\xi,$$

assuming two couple of images as N_1 corresponding to $\mathrm{T}_{N_1(x,t)}$ and N_2 corresponding to $\mathrm{T}_{N_2(x,t)}$ such that

$$\mathrm{T}_{N_1}(x,t) = N_0(x) + \int_0^t \left(d_N N_{1xx} + rN_1(x,\xi)\left(\frac{N_1(x,\xi)}{M}-1\right) \times \left(1-\frac{N_1(x,\xi)}{K}\right) - \frac{qN_1(x,\xi)E(x,\xi)}{k+N_1(x,\xi)}\right)d\xi, \quad (13)$$

and

$$\mathrm{T}_{N_2}(x,t) = N_0(x) + \int_0^t \left(d_N N_{2xx} + rN_2(x,\xi)\left(\frac{N_2(x,\xi)}{M}-1\right) \times \left(1-\frac{N_2(x,\xi)}{K}\right) - \frac{qN_2(x,\xi)E(x,\xi)}{k+N_2(x,\xi)}\right)d\xi, \quad (14)$$

subtract (14) from (13) we have

$$\begin{aligned}\mathrm{T}_{N_1}(x,t) - \mathrm{T}_{N_2}(x,t) &= \int_0^t \left(d_N N_{1xx} + rN_1(x,\xi)\left(\frac{N_1(x,\xi)}{M}-1\right) \times \left(1-\frac{N_1(x,\xi)}{K}\right) - \frac{qN_1(x,\xi)E(x,\xi)}{k+N_1(x,\xi)}\right)d\xi \\ &\quad - \int_0^t \left(d_N N_{2xx} + rN_2(x,\xi)\left(\frac{N_2(x,\xi)}{M}-1\right) \times \left(1-\frac{N_2(x,\xi)}{K}\right) - \frac{qN_2(x,\xi)E(x,\xi)}{k+N_2(x,\xi)}\right)d\xi,\end{aligned}$$

$$\begin{aligned}\mathrm{T}_{N_1}(x,t) - \mathrm{T}_{N_2}(x,t) &= \int_0^t d_N(N_{1xx}-N_{2xx}) + r\left(N_1\left(\frac{N_1}{M}-1\right)\left(1-\frac{N_1}{K}\right) - N_2\left(\frac{N_2}{M}-1\right)\left(1-\frac{N_2}{K}\right)\right) \\ &\quad + \left(\frac{qN_2E}{k+N_2} - \frac{pqN_1E}{k+N_1}\right)d\xi,\end{aligned}$$

using the mean value theorem from fundamental calculus we have

$$\begin{aligned}\mathrm{T}_{N_1}(x,t) - \mathrm{T}_{N_2}(x,t) = \int_0^t & d_N(N_{1xx}-N_{2xx}) \\ & + rN'(\kappa_3)(N_1-N_2) \\ & + qN'(\kappa_4)(N_1-N_2)Ed\xi,\end{aligned}$$

where $N'(\kappa_3)$ and $N'(\kappa_3)$ are constant, taking norm on both sides we get

$$\begin{aligned}||\mathrm{T}_{N_1}(x,t) - \mathrm{T}_{N_2}(x,t)|| = \int_0^t & |d_N|||N_{1xx}-N_{2xx}|| \\ & + |r||N'(\kappa_3)|||N_1-N_2|| \\ & + |qN'(\kappa_4)|||N_1-N_2||||E||d\xi,\end{aligned}$$

$$\begin{aligned}||\mathrm{T}_{N_1}(x,t) - \mathrm{T}_{N_2}(x,t)|| = \int_0^t & |d_N|\kappa_5 + |r||N'(\kappa_3)| \\ & + |qN'(\kappa_4)|(r^*+b)d\xi||N_1-N_2||,\end{aligned}$$

$$\begin{aligned}||\mathrm{T}_{N_1}(x,t) - \mathrm{T}_{N_2}(x,t)|| = & |d_N|\kappa_5 + |r||N'(\kappa_3)| \\ & + |qN'(\kappa_4)|(r^*+b)L||N_1-N_2||,\end{aligned}$$

using Lipchitz inequality for contraction with constant 1 we have

$$|d_N|\kappa_5 + |r||N'(\kappa_3)| + |qN'(\kappa_4)|(r^*+b)L < 1$$

so

$$L_{N^c} < \frac{1}{|d_N|\kappa_5 + |r||N'(\kappa_3)| + |qN'(\kappa_4)|(r^*+b)}$$

which inequality is a bounded condition of contraction for operator (9), similarly we find the contraction condition for operator (10) such that

$$L_{E^c} < \frac{1}{|d_E|\kappa_7 + |\alpha pqE'(\kappa_6)|(r^* + b) + |\alpha c|}$$

Lemma 2 Under the conditions of L_{N^c} and L_{E^c} the fixed point operators (9)–(10) have a unique fixed point in the closed and convex subsets B_N and B_E of space $C[0, \frac{1}{|d_N|\kappa_5+|r||N'(\kappa_3)|+|qN'(\kappa_4)|(r^*+b)}]$ and $C[0, \frac{1}{|d_E|\kappa_7+|\alpha pqE'(\kappa_6)|(r^*+b)+|\alpha c|}]$.

Theorem 3 If lemmas (1) and (2) are satisfied under a Banach space of all continuous solutions functions then there exists a guaranteed unique solution for the system (5–6) (Shahzad et al. 2024).

Numerical methods

The approximate solutions of nonlinear PDEs are carried out by various numerical techniques. The numerical techniques are backward Euler (BE) scheme and the implicit finite difference (IFD) scheme is developed for a given model. Let us assume that we divide the spatial and temporal coordinates as follows:

$x_n = n\Delta x, n = 0, 1, 2, 3, \ldots, \boldsymbol{M}$,
$t_m = m\Delta t, m = 0, 1, 2, 3, \ldots, \boldsymbol{N}$,

where $\Delta x, \Delta t$ show the space time stepsizes. For this computational study, one of them is the implicit scheme, and the appropriate approximations on Eqs. (1)–(2)are given as

$$\frac{\partial N}{\partial t} \approx \frac{N_n^{m+1} - N_n^m}{\Delta t}, \quad \frac{\partial^2 N}{\partial x^2} \approx \frac{N_{n+1}^{m+1} - 2N_n^{m+1} + N_{n-1}^{m+1}}{\triangle x^2},$$
$$\frac{\partial E}{\partial t} \approx \frac{E_n^{m+1} - E_n^m}{\Delta t}, \quad \frac{\partial^2 E}{\partial x^2} \approx \frac{E_{n+1}^{m+1} - 2E_n^{m+1} + E_{n-1}^{m+1}}{\triangle x^2}, -N \approx -N_n^{m+1}.$$

By doing some basic calculations, the IFD scheme is written as

$$-\lambda_1 N_{n+1}^{m+1} + \left(1 + 2\lambda_1 + r\Delta t + \frac{r(N_n^m)^2}{KM}\Delta t + \frac{qE_n^m}{k + N_n^m}\Delta t\right)N_n^{m+1} - \lambda_1 N_{n-1}^{m+1} = N_n^m + \frac{r(N_n^m)^2}{M}\Delta t + \frac{r(N_n^m)^2}{K}\Delta t, \tag{15}$$

$$-\lambda_2 E_{n+1}^{m+1} + (1 + 2\lambda_2 + \alpha c\Delta t)E_n^{m+1} - \lambda_2 E_{n-1}^{m+1} = E_n^m\left(1 + \frac{\alpha pqN_n^m}{k + N_n^m}\Delta t\right). \tag{16}$$

The Eqs. (15)–(16) are the required Implicit finite difference scheme for the given model.

For this study another computational scheme is the backward Euler scheme and the appropriate approximations for this are given as

$$\frac{\partial N}{\partial t} \approx \frac{N_n^{m+1} - N_n^m}{\Delta t}, \quad \frac{\partial^2 N}{\partial x^2} \approx \frac{N_{n+1}^{m+1} - 2N_n^m + N_{n-1}^{m+1}}{\triangle x^2},$$
$$\frac{\partial E}{\partial t} \approx \frac{E_n^{m+1} - E_n^m}{\Delta t}, \quad \frac{\partial^2 E}{\partial x^2} \approx \frac{E_{n+1}^{m+1} - 2E_n^m + E_{n-1}^{m+1}}{\triangle x^2}.$$

by using these approximations in Eqs. (1)–(2)the backward Euler scheme is given as

$$-\lambda_1 N_{n+1}^{m+1} + N_n^{m+1}(1 + 2\lambda_1) - \lambda_1 N_{n-1}^{m+1} = N_n^m\left(1 - r\Delta t - \frac{qE_n^m}{k + N_n^m}\Delta t\right) + \Delta t(N_n^m)^2\left(\frac{r}{M} + \frac{r}{k}\right) - \frac{r(N_n^m)^3}{KM}\Delta t. \tag{17}$$

$$-\lambda_2 E_{n+1}^{m+1} + E_n^{m+1}(1 + 2\lambda_2) - \lambda_2 E_{n-1}^{m+1} = E_n^m\left(1 - \alpha c\Delta t + \frac{\alpha pqN_n^m}{k + N_n^m}\Delta t\right). \tag{18}$$

The Eqs. (17)–(18) are the required backward Euler scheme for the under consideration model. where $\frac{d_N\Delta t}{\Delta x^2} = \lambda_1, \frac{d_E\Delta t}{\Delta x^2} = \lambda_2$.

The numerical solution of a given model is analyzed by two schemes one is a backward Euler and the other is an Implicit finite difference scheme. The underlying model is a population model and it preserves some dynamical properties. So, a solution that preserves all such properties is suitable for the population models. For this reason, we are considering the implicit finite difference scheme which also has dynamic properties.

Implicit finite difference scheme

In situations where accuracy is crucial and computational cost is an issue, such as in unsteady flow simulations, implicit finite difference schemes are useful because they enable larger time steps in simulations without compromising stability. So we chose the Implicit finite difference scheme for the fish harvesting model because it generally gives a solution to the problems of the type having no restriction on the time step. The important aspect of this scheme is to give a simultaneous solution to the problem because it enables information from the entire range to affect the solution at any point in time. Moreover, as we compare to explicit numerical schemes, where the time step is much larger. According to von Neumann stability analyses

conducted by Liggett and Cunge and Fread, the implicit scheme is unconditionally stable.

The Implicit finite difference scheme is written as

$$-\lambda_1 N_{n+1}^{m+1}+\left(1+2\lambda_1+r\Delta t+\frac{r(N_n^m)^2}{KM}\Delta t+\frac{qE_n^m}{k+N_n^m}\Delta t\right)N_n^{m+1} -\lambda_1 N_{n-1}^{m+1}=N_n^m+\frac{r(N_n^m)^2}{M}\Delta t+\frac{r(N_n^m)^2}{K}\Delta t, \tag{19}$$

$$-\lambda_2 E_{n+1}^{m+1}+(1+2\lambda_2+\alpha c\Delta t)E_n^{m+1}-\lambda_2 E_{n-1}^{m+1} =E_n^m\left(1+\frac{\alpha pqN_n^m}{k+N_n^m}\Delta t\right). \tag{20}$$

Stability

We used linear stability analysis in the system of Eqs. (15)–(16) and we first put $N_n^m=\phi(t)e^{i\omega x}$, $N_n^{m+1}=\phi(t+\Delta t)e^{i\omega x}$, $N_{n+1}^{m+1}=\phi(t+\Delta t)e^{i\omega(x+\Delta x)}$ and $N_{n-1}^{m+1}=\phi(t+\Delta t)e^{i\omega(x-\Delta x)}$. By linearization of Eq. (15) and eliminating the nonlinear terms, we get

$$-\lambda_1 N_{n+1}^{m+1}+N_n^{m+1}(1+2\lambda_1+r\Delta t)-\lambda_1 N_{n-1}^{m+1}=N_n^m. \tag{21}$$

$$-\lambda_1(\phi_1(t+\Delta t)e^{i\omega(x+\Delta x)}) +\phi_1(t+\Delta t)e^{i\omega x}(1+2\lambda_1+r\Delta t)-\lambda_1(\phi_1(t+\Delta t)e^{i\omega(x-\Delta x)}) =\phi_1(t)e^{i\omega x}. \tag{22}$$

$$\phi_1(t+\Delta t)e^{i\omega x}(1+2\lambda_1+r\Delta t) =\phi(t)_1 e^{i\omega x}+\lambda_1\phi_1(t)e^{i\omega(x-\Delta x)}+\lambda_1\phi(t)_1 e^{i\omega(x+\Delta x)}, \tag{23}$$

$$\phi_1(t+\Delta t)e^{i\omega x}(1+2\lambda_1+r\Delta t) =\phi_1(t)e^{i\omega x}+\lambda_1\phi(t)(2\cos(\omega\Delta x))e^{i\omega x}, \tag{24}$$

$$\left|\frac{\phi_1(t+\Delta t)}{\phi_1(t)}\right|=\left|\frac{1+2\lambda_1\cos(\omega\Delta x)}{(1+2\lambda_1+r\Delta t)}\right|\le 1. \tag{25}$$

Similar process applied for (16)

$$\left|\frac{\phi_2(t+\Delta t)}{\phi_2(t)}\right|=\left|\frac{1+2\lambda_2\cos(\omega\Delta x)}{(1+2\lambda_2+\alpha c\Delta t)}\right|\le 1. \tag{26}$$

From (25) and (26) it is verified that proposed implicit schemes (15)and (16) are von Neumann stable.

Consistency for scheme

Definition 1 A computational is called consistent if $T(x,t)\to 0$ as $\triangle x\to 0, \triangle t\to 0$.

The consistency of the implicit FD scheme is analyzed here. The scheme is given as

$$-\lambda_1 N_{n+1}^{m+1}+\left(1+2\lambda_1+r\Delta t+\frac{r(N_n^m)^2}{KM}\Delta t+\frac{qE_n^m}{k+N_n^m}\Delta t\right)N_n^{m+1} -\lambda_1 N_{n-1}^{m+1}=N_n^m+\frac{r(N_n^m)^2}{M}\Delta t+\frac{r(N_n^m)^2}{K}\Delta t,$$

$$-\lambda_2 E_{n+1}^{m+1}+(1+2\lambda_2+\alpha c\Delta t)E_n^{m+1}-\lambda_2 E_{n-1}^{m+1} =E_n^m\left(1+\frac{\alpha pqN_n^m}{k+N_n^m}\Delta t\right).$$

The terms involved in the scheme are expanded by the Taylor series:

$$\begin{aligned}
N_n^{m+1} =& N_n^m+\Delta t\frac{\partial N_m^n}{\partial t}+\frac{\Delta t^2}{2!}\frac{\partial^2 N_n^m}{\partial t^2}+\frac{\Delta t^3}{3!}\frac{\partial^3 N_n^m}{\partial t^3}+\cdots,\\
N_{n+1}^{m+1} =& N_n^m+\Delta t\frac{\partial N_n^m}{\partial t}+\Delta x\frac{\partial N_n^m}{\partial x}+\frac{\Delta t^2}{2!}\frac{\partial^2 N_n^m}{\partial t^2}\\
&+\frac{\Delta x^2}{2!}\frac{\partial^2 N_n^m}{\partial x^2}+\Delta t\Delta x\frac{\partial^2 N_n^m}{\partial x\partial t}+\cdots,\\
N_{n-1}^{m+1} =& N_n^m+\Delta t\frac{\partial N_n^m}{\partial t}-\Delta x\frac{\partial N_n^m}{\partial x}+\frac{\Delta t^2}{2!}\frac{\partial^2 N_n^m}{\partial t^2}\\
&+\frac{\Delta x^2}{2!}\frac{\partial^2 N_n^m}{\partial x^2}-\Delta t\Delta x\frac{\partial^2 N_n^m}{\partial x\partial t}+\cdots,\\
E_n^{m+1} =& E_n^m+\Delta t\frac{\partial E_n^m}{\partial t}+\frac{\Delta t^2}{2!}\frac{\partial^2 E_n^e}{\partial t^2}\\
&+\frac{\Delta t^3}{3!}\frac{\partial^3 E_n^m}{\partial t^3}+\cdots,\\
E_{n+1}^{m+1} =& E_n^m+\Delta t\frac{\partial E_n^m}{\partial t}+\Delta x\frac{\partial E_n^m}{\partial x}+\frac{\Delta t^2}{2!}\frac{\partial^2 E_n^m}{\partial t^2}\\
&+\frac{\Delta x^2}{2!}\frac{\partial^2 E_n^m}{\partial x^2}+\Delta t\Delta x\frac{\partial^2 E_n^m}{\partial x\partial t}+\cdots,\\
E_{n-1}^{m+1} =& E_n^m+\Delta t\frac{\partial E_n^m}{\partial t}-\Delta x\frac{\partial E_n^m}{\partial x}\\
&+\frac{\Delta t^2}{2!}\frac{\partial^2 E_n^m}{\partial t^2}+\frac{\Delta x^2}{2!}\frac{\partial^2 E_n^m}{\partial x^2}-\Delta t\Delta x\frac{\partial^2 E_n^m}{\partial x\partial t}+\cdots,
\end{aligned}$$

By using above Taylor series expansion of $N_{n+1}^{m+1}, N_n^{m+1}, N_{n+1}^m$ in the equation

$$
\begin{aligned}
&-\lambda_1\left(N_n^m+\Delta t\frac{\partial N_n^m}{\partial t}+\Delta x\frac{\partial N_n^m}{\partial x}+\frac{\Delta t^2}{2!}\frac{\partial^2 N_n^m}{\partial t^2}\right.\\
&\left.+\frac{\Delta x^2}{2!}\frac{\partial^2 N_n^m}{\partial x^2}+\Delta t\Delta x\frac{\partial^2 N_n^m}{\partial x\partial t}\right)\\
&+\left(1+2\lambda_1+r+\frac{r(N_n^m)^2}{KM}+\frac{qE_n^m}{k+N_n^m}\right)\\
&\times\left(N_n^m+\Delta t\frac{\partial N_m^n}{\partial t}+\frac{\Delta t^2}{2!}\frac{\partial^2 N_n^m}{\partial t^2}+\frac{\Delta t^3}{3!}\frac{\partial^3 N_n^m}{\partial t^3}+\cdots\right)\\
&-\lambda_1\left(N_n^m+\Delta t\frac{\partial N_n^m}{\partial t}-\Delta x\frac{\partial N_n^m}{\partial x}+\frac{\Delta t^2}{2!}\frac{\partial^2 N_n^m}{\partial t^2}\right.\\
&\left.+\frac{\Delta x^2}{2!}\frac{\partial^2 N_n^m}{\partial x^2}-\Delta t\Delta x\frac{\partial^2 N_n^m}{\partial x\partial t}+\cdots\right)\\
&=N_n^m+\frac{r(N_n^m)^2}{M}+\frac{r(N_n^m)^2}{K},
\end{aligned}
\tag{27}
$$

after simplification of the equation, we get

$$
\frac{\partial N}{\partial t}=d_N N_{xx}+rN\left(\frac{N}{M}-1\right)\left(1-\frac{N}{K}\right)-\frac{pqNE}{k+N},
\tag{28}
$$

A similar process was applied to the second equation

$$
\frac{\partial E}{\partial t}=d_E E_{xx}+\alpha\left(\frac{pqNE}{k+N}-cE\right).
\tag{29}
$$

Equations (28)and (29) proved that IFD method is consistent with $\triangle x$ and $\triangle t\to 0$.

Positivity of implicit scheme

To show that the IFD scheme preserves the positivity, M-matrix theory and Induction method (Fujimoto and Ranade 2004; Ahmed et al. 2021, 2018) is used. We use Eqs. (15)–(16) as

$$
AN^{m+1}=L,
\tag{30}
$$

$$
BE^{m+1}=M,
\tag{31}
$$

Both L and M are column matrices and A and B are the square matrices of order $N+1$.

$$
A=\begin{bmatrix}
m_1 & m_2 & 0 & & 0 & 0 & 0\\
m_3 & m_1 & m_3 & \cdots & 0 & 0 & 0\\
0 & m_3 & m_1 & & 0 & 0 & 0\\
 & \vdots & & \ddots & & \vdots & \\
0 & 0 & 0 & & m_1 & m_3 & 0\\
0 & 0 & 0 & & m_3 & m_1 & m_3\\
0 & 0 & 0 & \cdots & 0 & m_2 & m_1\\
, & & & & & &
\end{bmatrix}
$$

$$
B=\begin{bmatrix}
p_1 & p_2 & 0 & & 0 & 0 & 0\\
p_3 & p_1 & p_3 & \cdots & 0 & 0 & 0\\
0 & p_3 & p_1 & & 0 & 0 & 0\\
 & \vdots & & \ddots & & \vdots & \\
0 & 0 & 0 & & p_1 & p_3 & 0\\
0 & 0 & 0 & & p_3 & p_1 & p_1\\
0 & 0 & 0 & \cdots & 0 & p_2 & p_1\\
, & & & & & &
\end{bmatrix}
$$

The diagonal and non-diagonal entries of matrix A is $m_1=1+2\lambda_1+r+\frac{rN_n^m}{KM}+\frac{pqE_n^m}{k+N}, m_2=-\lambda_1$ and $m_3=-\lambda_1$ The diagonal and non-diagonal entries of matrix B is $p_1=1+2\lambda_2+\alpha c, p_2=-\lambda_2$ and $p_3=-\lambda_2$ where $\lambda_1=\frac{\Delta t d_N}{\Delta x^2}$, $\lambda_2=\frac{\Delta t d_E}{\Delta x^2}$. As it is given $N_n^0\geq 0$ and $E_n^0\geq 0$, this implies the value of the m_1 is positive, also the values of the p_1 are positive. As m_2, m_3, p_2, p_3 have negative values, the matrix A, and B are strictly dominant. So, using the all above arguments leads towards that matrices A and B are the M-matrices. Hence, the given matrices A and B are nonsingular. So, the Eqs. (30) and (31) takes the following form

$$
N^{m+1}=A^{-1}L,
\tag{32}
$$

$$
E^{m+1}=B^{-1}M,
\tag{33}
$$

It is the assumption that $N^m>0$ and $E^m>0$, and the matrices A and B are the M-matrices and all the entries of their inverses are positive. So, $N^{m+1}>0, E^{m+1}>0$, and with the help of the Induction method, our scheme is positive.

Backward Euler method

For numerical solutions of any problem backward Euler method has much importance so we use this method for solving the ordinary differential equation for the given model because it provides unconditional stability and can handle stiff problems that the other methods such as Forward Euler method finds difficult to handle. Although the backward Euler method is stable, its accuracy is limited because it is a first-order method. Smaller time steps are required for greater accuracy because the error in the solution is proportional to the time step.

The backward Euler scheme for the given system is given as

$$
\begin{aligned}
&-\lambda_1 N_{n+1}^{m+1} + N_n^{m+1}(1+2\lambda_1) - \lambda_1 N_{n-1}^{m+1} \\
&\quad = N_n^m\left(1 - r\Delta t - \frac{qE_n^m}{k+N_n^m}\Delta t\right) + (N_n^m)^2\left(\frac{r}{M}+\frac{r}{k}\right)\Delta t. \\
&-\lambda_2 E_{n+1}^{m+1} + E_n^{m+1}(1+2\lambda_2) - \lambda_2 E_{n-1}^{m+1} \\
&\quad = E_n^m\left(1 - \alpha c\Delta t + \frac{\alpha pqN_n^m}{k+N_n^m}\Delta t\right).
\end{aligned}
$$

Stability

To check the linear stability of the system we used Von Neumann stability analysis and ignoring the non-linear terms of the system of equations, we first put $N_n^m = \phi(t)e^{i\omega x}$, $N_n^{m+1} = \phi(t+\Delta t)e^{i\omega x}$, $N_{n+1}^{m+1} = \phi(t+\Delta t)e^{i\omega(x+\Delta x)}$ and $N_{n-1}^{m+1} = \phi(t+\Delta t)e^{i\omega(x-\Delta x)}$

$$
-\lambda_1 N_{n+1}^{m+1} + N_n^{m+1}(1+2\lambda_1) - \lambda_1 N_{n-1}^{m+1} = N_n^m(1 - r\Delta t). \quad (34)
$$

substituting the above values, we have

$$
\begin{aligned}
&-\lambda_1(\Phi_1(t+\Delta t)e^{i\omega(x+\Delta x)}) + \Phi_1(t+\Delta t)e^{i\omega x}(1+2\lambda_1) \\
&\quad -\lambda_1(\Phi_1(t+\Delta t)e^{i\omega(x-\Delta x)}) = \Phi_1(t)e^{i\omega x}(1 - r\Delta t).
\end{aligned} \quad (35)
$$

$$
\begin{aligned}
&\Phi_1(t+\Delta t)e^{i\omega x}((1+2\lambda_1) - \lambda_1(2cos(\omega\Delta x))) \\
&\quad = \Phi_1(t)e^{i\omega x}(1 - r\Delta t),
\end{aligned} \quad (36)
$$

$$
\left|\frac{\Phi_1(t+\Delta t)}{\Phi_1(t)}\right| = \left|\frac{(1-r\Delta t)}{1+2\lambda_1 - 2\lambda_1(1-\sin^2(\frac{\omega\Delta x}{2}))}\right| \le 1, \quad (37)
$$

similarly

$$
\left|\frac{\Phi_1(t+\Delta t)}{\Phi_1(t)}\right| = \left|\frac{(1-\alpha c\Delta t)}{1+2\lambda_2 - 2\lambda_2(1-\sin^2(\frac{\omega\Delta x}{2}))}\right| \le 1, \quad (38)
$$

It is verified that the backward Euler scheme is von Neumann stable.

Consistency for preserving positivity

The consistency of the backward Euler scheme is given as

$$
\begin{aligned}
&-\lambda_1 N_{n+1}^{m+1} + N_n^{m+1}(1+2\lambda_1) - \lambda_1 N_{n-1}^{m+1} \\
&\quad = N_n^m\left(1 - r\Delta t - \frac{qE_n^m}{k+N_n^m}\Delta t\right) + \Delta t(N_n^m)^2 \\
&\qquad \times\left(\frac{r}{M}+\frac{r}{k}\right) - \frac{r(N_n^m)^3}{KM}\Delta t. \\
&-\lambda_2 E_{n+1}^{m+1} + E_n^{m+1}(1+2\lambda_2) - \lambda_2 E_{n-1}^{m+1} \\
&\quad = E_n^m(1 - \alpha c\Delta t + \frac{\alpha pqN_n^m}{k+N_n^m}\Delta t).
\end{aligned}
$$

The involved terms are expanded with the help of the Taylor series:

$$
\begin{aligned}
N_n^{m+1} =& N_n^m + \Delta t\frac{\partial N_m^n}{\partial t} + \frac{\Delta t^2}{2!}\frac{\partial^2 N_n^m}{\partial t^2} + \frac{\Delta t^3}{3!}\frac{\partial^3 N_n^m}{\partial t^3} + \cdots, \\
N_{n+1}^{m+1} =& N_n^m + \Delta t\frac{\partial N_n^m}{\partial t} + \Delta x\frac{\partial N_n^m}{\partial x} + \frac{\Delta t^2}{2!}\frac{\partial^2 N_n^m}{\partial t^2} \\
&+ \frac{\Delta x^2}{2!}\frac{\partial^2 N_n^m}{\partial x^2} + \Delta t\Delta x\frac{\partial^2 N_n^m}{\partial x\partial t} + \cdots, \\
N_{n-1}^{m+1} =& N_n^m + \Delta t\frac{\partial N_n^m}{\partial t} - \Delta x\frac{\partial N_n^m}{\partial x} + \frac{\Delta t^2}{2!}\frac{\partial^2 N_n^m}{\partial t^2} \\
&+ \frac{\Delta x^2}{2!}\frac{\partial^2 N_n^m}{\partial x^2} - \Delta t\Delta x\frac{\partial^2 N_n^m}{\partial x\partial t} + \cdots, \\
E_n^{m+1} =& E_n^m + \Delta t\frac{\partial E_n^m}{\partial t} + \frac{\Delta t^2}{2!}\frac{\partial^2 E_n^e}{\partial t^2} \\
&+ \frac{\Delta t^3}{3!}\frac{\partial^3 E_n^m}{\partial t^3} + \cdots, \\
E_{n+1}^{m+1} =& E_n^m + \Delta t\frac{\partial E_n^m}{\partial t} + \Delta x\frac{\partial E_n^m}{\partial x} + \frac{\Delta t^2}{2!}\frac{\partial^2 E_n^m}{\partial t^2} \\
&+ \frac{\Delta x^2}{2!}\frac{\partial^2 E_n^m}{\partial x^2} + \Delta t\Delta x\frac{\partial^2 E_n^m}{\partial x\partial t} + \cdots, \\
E_{n-1}^{m+1} =& E_n^m + \Delta t\frac{\partial E_n^m}{\partial t} - \Delta x\frac{\partial E_n^m}{\partial x} + \frac{\Delta t^2}{2!}\frac{\partial^2 E_n^m}{\partial t^2} + \frac{\Delta x^2}{2!}\frac{\partial^2 E_n^m}{\partial x^2} \\
&- \Delta t\Delta x\frac{\partial^2 E_n^m}{\partial x\partial t} + \cdots,
\end{aligned}
$$

By using above Taylor series expansion of $N_{n+1}^{m+1}, N_n^{m+1}, N_{n+1}^m$ in the equation

$$
\begin{aligned}
&-\lambda_1\Bigg(N_n^m+\Delta t\frac{\partial N_n^m}{\partial t}+\Delta x\frac{\partial N_n^m}{\partial x}+\frac{\Delta t^2}{2!}\frac{\partial^2 N_n^m}{\partial t^2}\\
&\quad+\frac{\Delta x^2}{2!}\frac{\partial^2 N_n^m}{\partial x^2}+\Delta t\Delta x\frac{\partial^2 N_n^m}{\partial x\partial t}+\cdots\Bigg)\\
&\quad+\left(N_n^m+\Delta t\frac{\partial N_m^n}{\partial t}+\frac{\Delta t^2}{2!}\frac{\partial^2 N_n^m}{\partial t^2}+\frac{\Delta t^3}{3!}\frac{\partial^3 N_n^m}{\partial t^3}+\cdots\right)\\
&\quad\times(1+2\lambda_1)-\lambda_1\Bigg(N_n^m+\Delta t\frac{\partial N_n^m}{\partial t}-\Delta x\frac{\partial N_n^m}{\partial x}+\frac{\Delta t^2}{2!}\frac{\partial^2 N_n^m}{\partial t^2}\\
&\quad+\frac{\Delta x^2}{2!}\frac{\partial^2 N_n^m}{\partial x^2}-\Delta t\Delta x\frac{\partial^2 N_n^m}{\partial x\partial t}+\cdots\Bigg)\\
&=N_n^m(1-r\Delta t-\frac{qE_n^m}{k+N_n^m}\Delta t)\\
&\quad+\Delta t(N_n^m)^2(\frac{r}{M}+\frac{r}{k})-\frac{r(N_n^m)^3}{KM}\Delta t.
\end{aligned}
\tag{39}
$$

After simplification, we get

$$
\frac{\partial N}{\partial t}=d_N N_{xx}+rN\left(\frac{N}{M}-1\right)\left(1-\frac{N}{K}\right)-\frac{pqNE}{k+N},
\tag{40}
$$

A similar process was applied to the second equation

$$
\frac{\partial E}{\partial t}=d_E E_{xx}+\alpha\left(\frac{pqNE}{k+N}-cE\right).
\tag{41}
$$

Thus from Eqs. (40) and (41) it is clear that the backward Euler scheme satisfies the consistency.

Results and discussion

As the fish harvesting model is a population-based model so we discuss it with the influence of the Allee effect. The Allee effect is the phenomenon whereby a population's growth rate decreases at low densities, which implies that the population may find it difficult to recover even if fishing pressure is decreased. Overfishing can cause a population crash when the Allee effect is present, and even with less fishing pressure, the population might not be able to recover. Scientists investigate the Allee effect and its consequences for fish harvesting using mathematical models. this model can give a better understanding of how the Allee effect interacts with various fishing techniques and environmental factors to affect population dynamics.

In this section, the theoretical results obtained in the above sections are verified with numerical simulations. The given model is

$$
N_t=d_N N_{xx}+rN\left(\frac{N}{M}-1\right)\left(1-\frac{N}{K}\right)-\frac{qNE}{k+N},
\tag{42}
$$

$$
E_t=d_E E_{xx}+\frac{\alpha pqNE}{k+N}-\alpha cE,
\tag{43}
$$

with initial data

$$
N(x,0)=70,\quad E(x,0)=40,
\tag{44}
$$

and having homogeneous Neumann boundary conditions. The numerical solution of a given model is analyzed by two schemes one is a backward Euler and the other is an Implicit finite difference scheme. The underlying model is a population model and it preserves some dynamical properties. So, a solution that preserves all such properties is suitable for the population models. For this reason, we are considering the implicit finite difference scheme which has dynamical properties. The under lying model has four equilibrium points as $E_1=(0,0)$, $E_2=(M,0)$, $E_3=(K,0)$ and $E_4=\left(\frac{kc}{pq-c},\frac{\beta pr(-\beta+K)(-M+\beta)}{cMK}\right)$, where $\beta=\frac{kc}{pq-c}$. The physical description of the above equilibriums is as follows,

- The equilibrium $E_1=(0,0)$ represents that there is no fish population and no effort can be applied to harvest them.
- The equilibrium $E_2=(M,0)$ represent that the fish population at its lowest level. So, with any effort applied to harvest them, the fish population will decrease and in the long term, it will extinct.
- The equilibrium point $E_3=(K,0)$ represents that the population is at its highest level then it becomes constant and no effort is applied to harvest
- The equilibrium $E_4=\left(\frac{kc}{pq-c},\frac{\beta pr(-\beta+K)(-M+\beta)}{cMK}\right)$ represent that population is at a high level and then decreases over time.

k	q	α	p	r	Δt	Δx	d_N	d_E
60	0.6	1	0.2	0.2	3000/3000	0.01	1	1

For a detailed study, we used MATLAB software for simulations. The values of the parameter for the initial population are taken as $M=5$, $k=50$, and $c=0.05$. In Figs. 1, 2, we noticed that in both schemes dynamical system is stable for a constant population when no fish population and no effort is applied to harvest them, which indicates that the fish

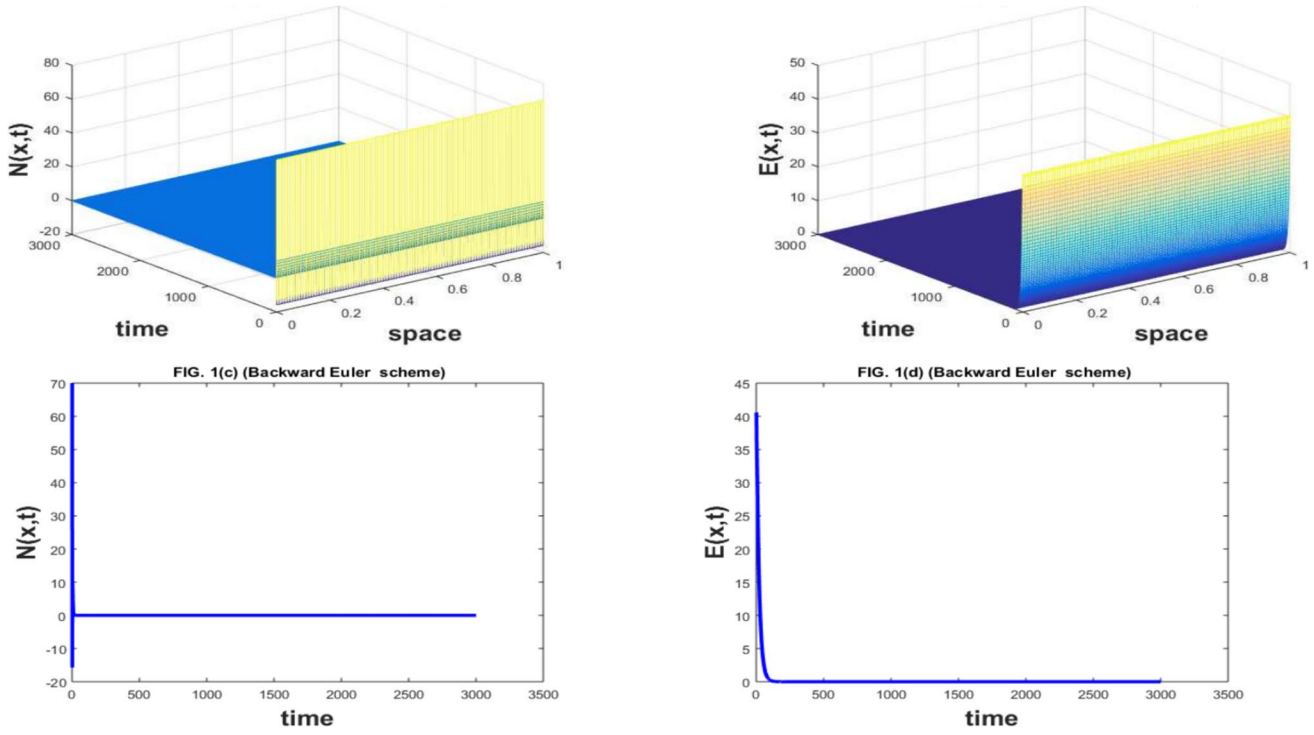

Fig. 1 The 3D and 2D diagrams of fish population and its harvesting by BE scheme for $M = 5, K = 50, c = 0.05$

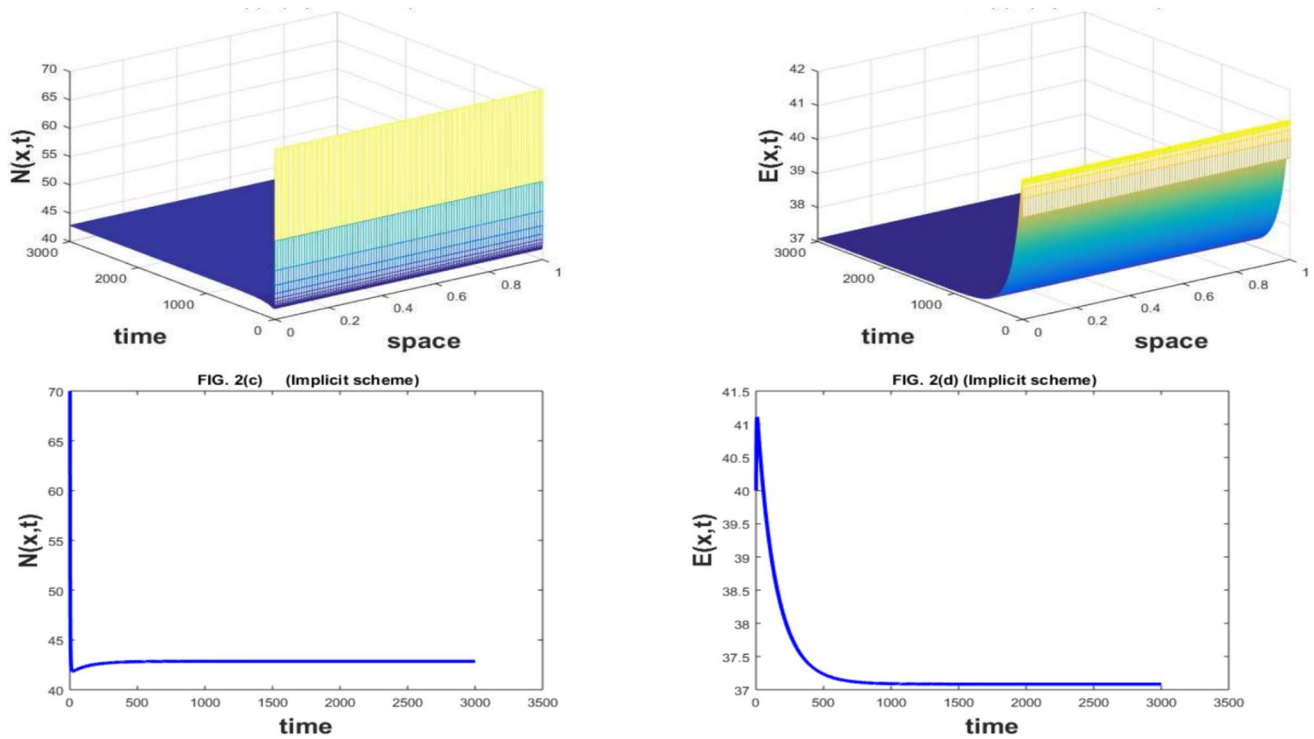

Fig. 2 The 3D and 2D diagrams of fish population and its harvesting by IFD scheme for $M = 5, K = 50, c = 0.05$

species are persisted for a long time and extinction occurs. The results gained by the backward Euler scheme possess negative behavior and such results are useless for population models. The results obtained by the scheme are positive, and consistent and preserve all the dynamical properties of a given model.

While at the second equilibrium point E_2 the fish species have not survived for a long time and it gives the lowest values which shows they might be eliminated through the harvesting rate. Since fish have some upbringing season we avoid harvesting during that time in Figs. 3, 4. It is noticed that at $c = 0.05$ it shows suitable results for the fish population surviving periodically and the fish population is extinct. To show the impact of harvesting, we draw the graph at equilibrium conditions. We've seen that at $c = 0.0614$, the maximum amount of fish may be harvested, in this starting population in Figs. 5 and 6. at the starting point of E_3 the fish population harvesting rate is so high and survived periodically that it shows constant behavior and no fish are harvested in Figs. 7, 8.

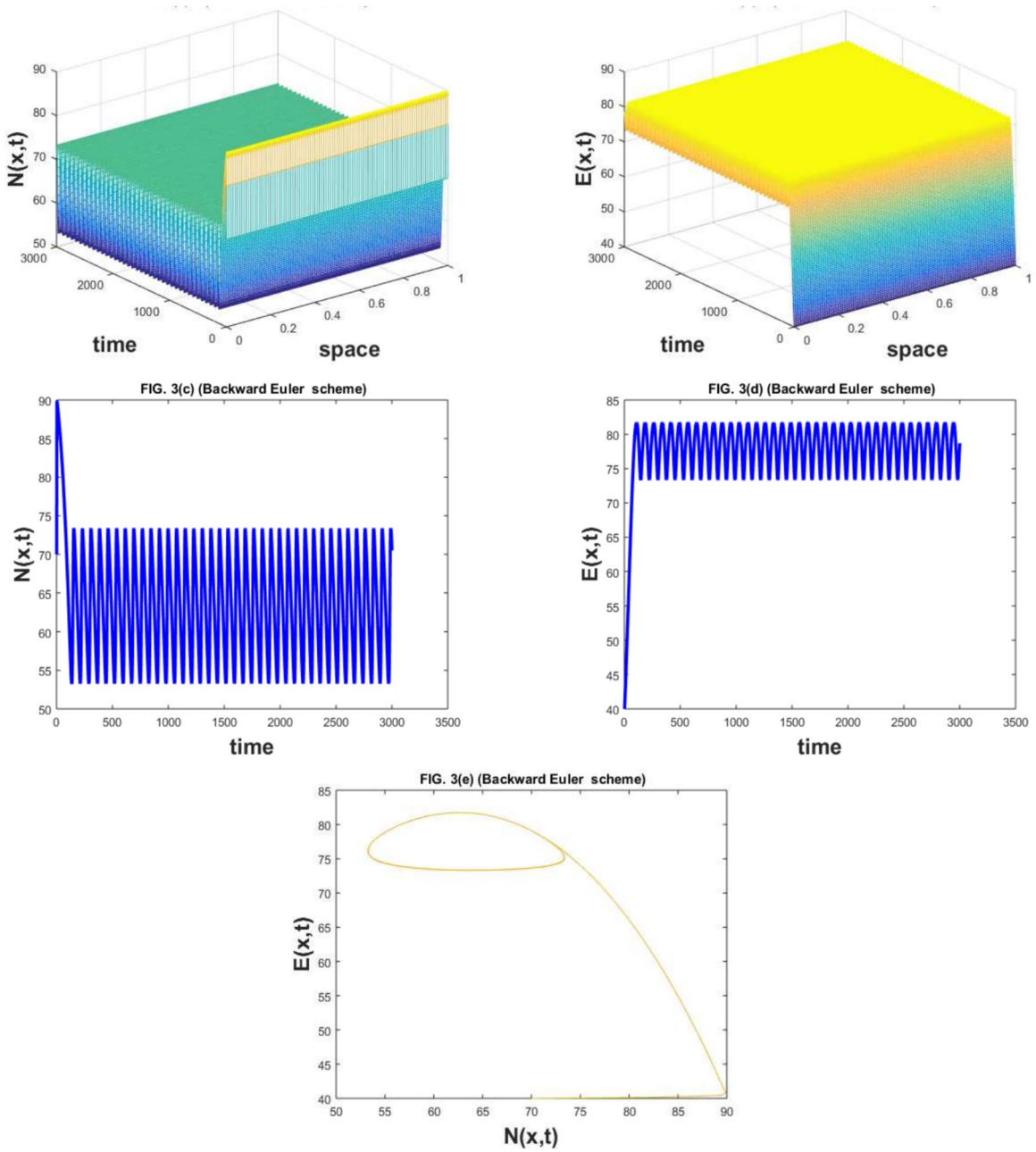

Fig. 3 The 3D and 2D diagrams of fish population and its harvesting by BE scheme for $M = 10, K = 100, c = 0.0614$

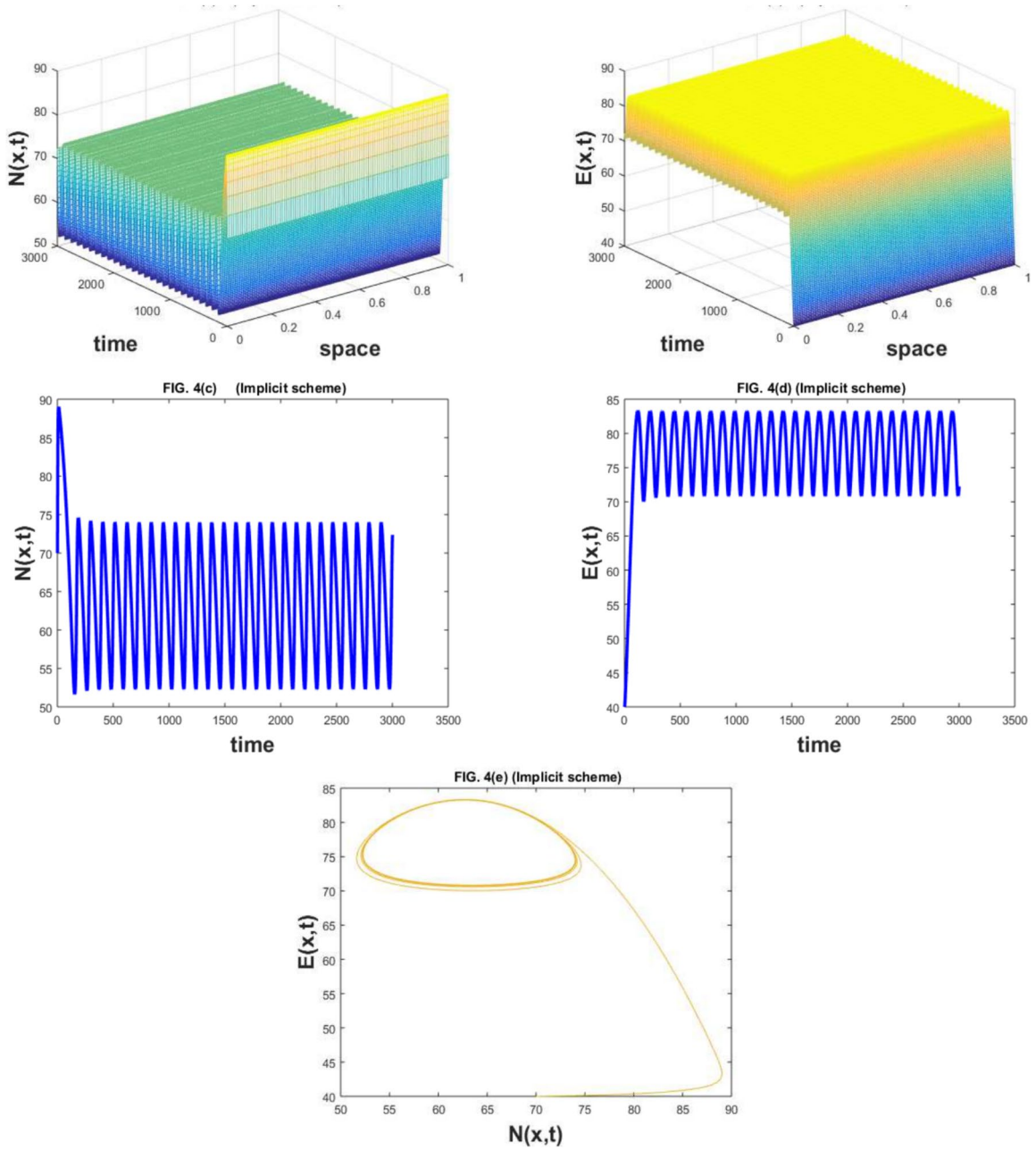

Fig. 4 The 3D and 2D diagrams of fish population and its harvesting by IFD scheme for $M = 10, K = 100, c = 0.0614$

At E_4 the fish harvesting rate is high and then it decreases and no effort is applied to harvest the fish population and shows stable behavior in Figs. 9, 10.

The underlying model is a population model and to gain the numerical solution is not a simple task. For this, we have used the two finite difference schemes, which are backward Euler and an implicit scheme. A qualitative analysis of the schemes is derived. The backward Euler scheme is von Neumann stable and consistent with the continuous model. The other scheme is also von Neumann stable and consistent with the underlying model. The positivity of the scheme is proved by using the M-matrices theory and induction technique. A test problem is used to validate the analytical results of the scheme. The numerical results obtained with the help of the backward Euler scheme are consistent, stable, and bounded behavior, but negative behavior is not biologically possible. However, the results obtained by an Implicit scheme are positive, bounded, stable, and consistent with the continuous system. All the essential properties of the continuous are preserved by the Implicit scheme. All the analytical results are validated by the numerical simulation.

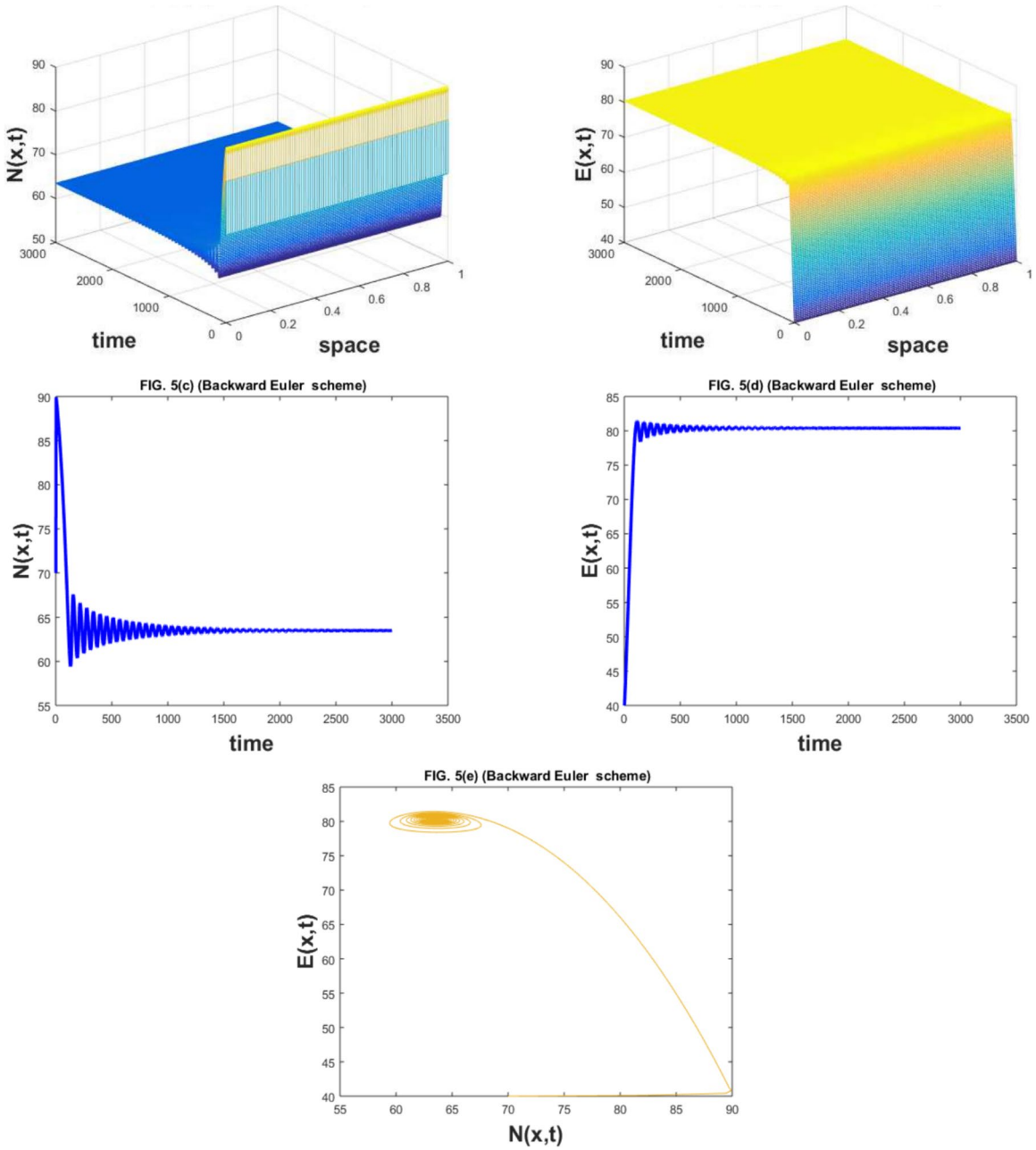

Fig. 5 The 3D and 2D diagrams of fish population and its harvesting by BE scheme for $M = 10, K = 100, c = 0.0617$

Conclusion

This manuscript deals with the fish harvesting model with the Allee effect and harvesting phenomena are represented by the Holling functional response of type II. The study of the underlying model is analyzed by the two time-efficient numerical methods. The existence of a unique solution for the underlying model is guaranteed with some a-priori estimates by using fixed point theory. The given model is a population model and its solutions have some specific properties i.e., consistent, bounded, positive, etc. The backward Euler is dynamically consistent with the given model, its linear stability is carried out and it is von Neumann stable. The Implicit finite difference scheme is also applied to the numerical results of the given model. The IFDS scheme is consistent with the dynamical system, the linear analysis is carried out and it is von Neumann stable. The positivity of the IFDS scheme is developed by the induction method. The given model has four equilibrium points. The simulations are drawn for the various values of the parameters by the backward Euler scheme and Implicit finite difference scheme. The

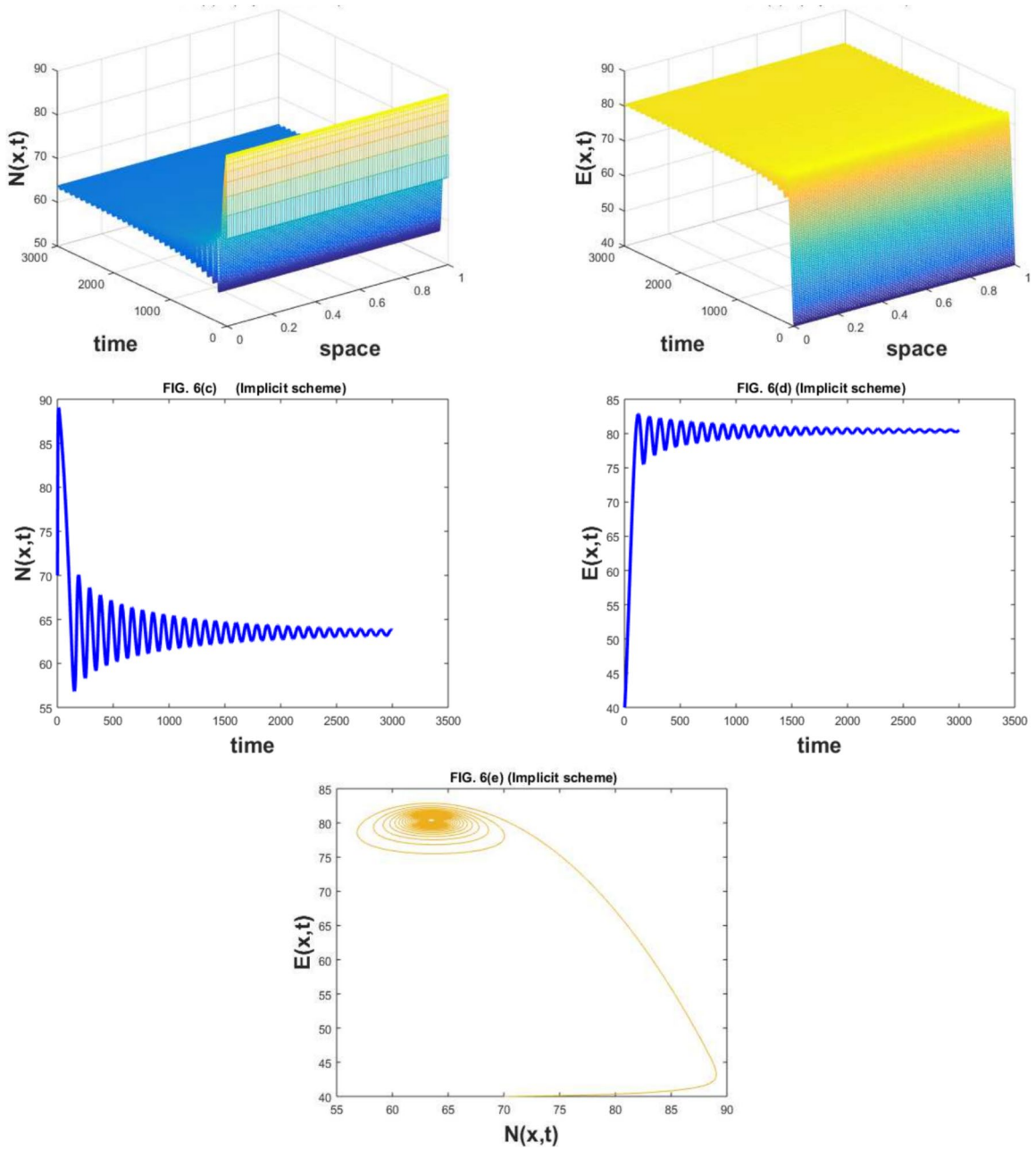

Fig. 6 The 3D and 2D diagrams of fish population and its harvesting by IFD scheme for $M = 10, K = 100, c = 0.0617$

results gained by the backward Euler scheme showed negative behavior and such behavior is not acceptable for population models. However, the results obtained by the IFD scheme showed positive behavior for the whole domain. This scheme preserves all properties of the continuous model such as positivity, bounded, and consistency. These results will help the researchers to use schemes that preserve the qualitative properties of the dynamical model in the future. As population and disease dynamics preserve some essential properties, so for their numerical solution it is necessary to contain all possible properties. In this manuscript, we have tried to use a scheme that preserves such properties. In the future, such structure-preserving solutions will be gained for the stochastic reaction-diffusion prey-predator models, stochastic reaction-diffusion epidemic models, and other emerging fields.

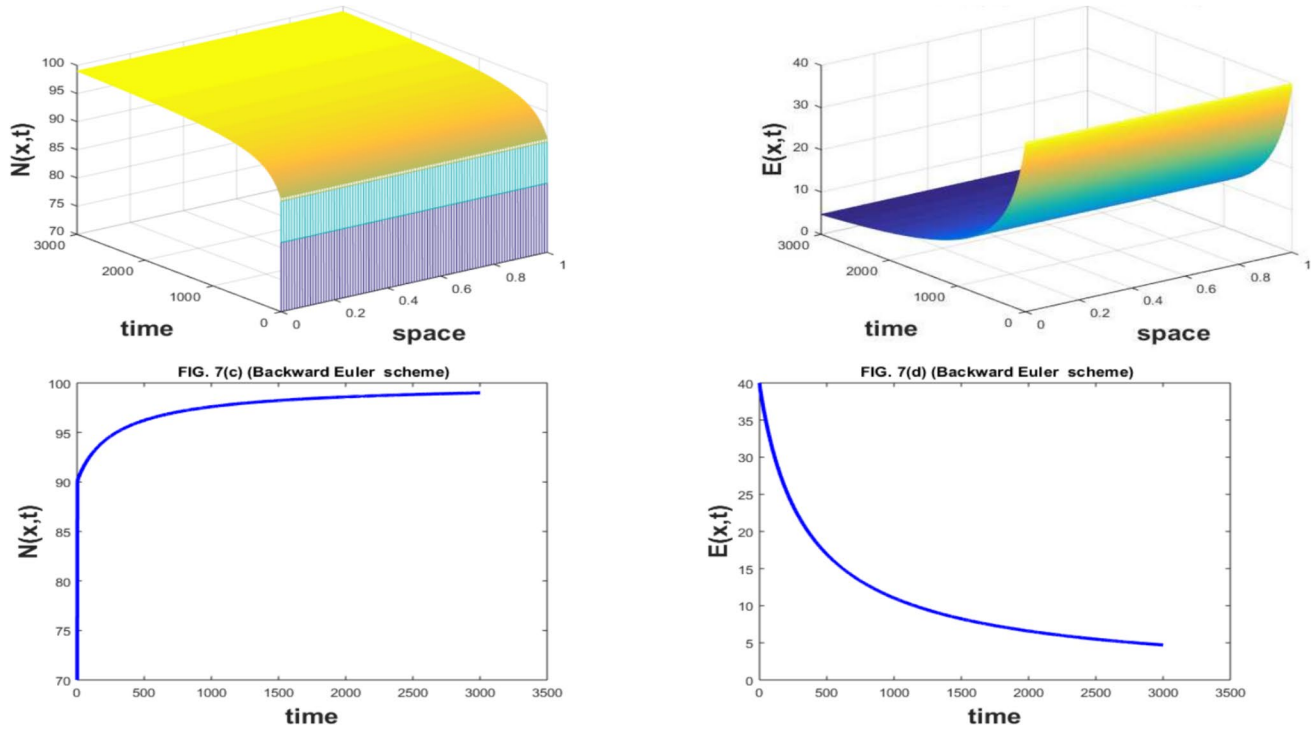

Fig. 7 The 3D and 2D diagrams of fish population and its harvesting by BE scheme for $M = 10, K = 100, c = 0.075$

Fig. 8 The 3D and 2D diagrams of fish population and its harvesting by IFD scheme for $M = 10, K = 100, c = 0.075$

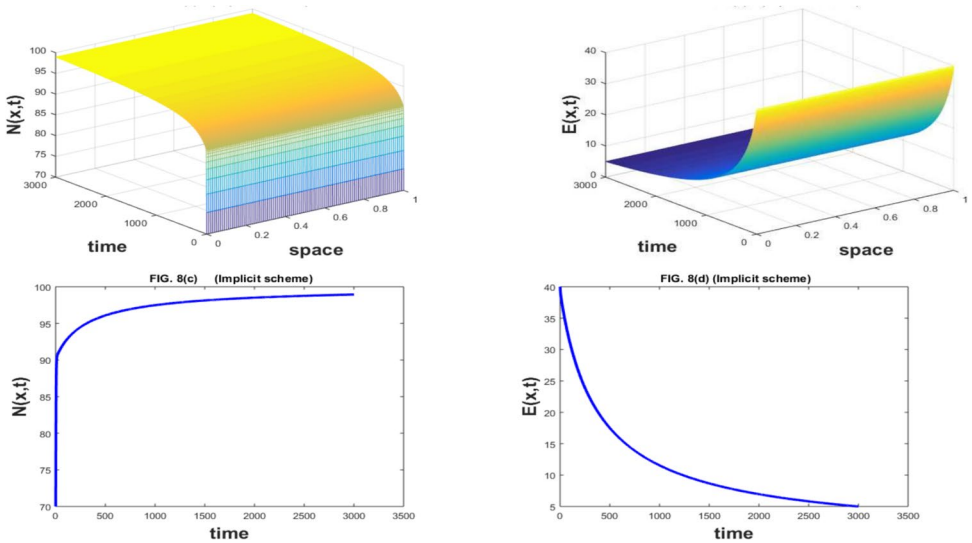

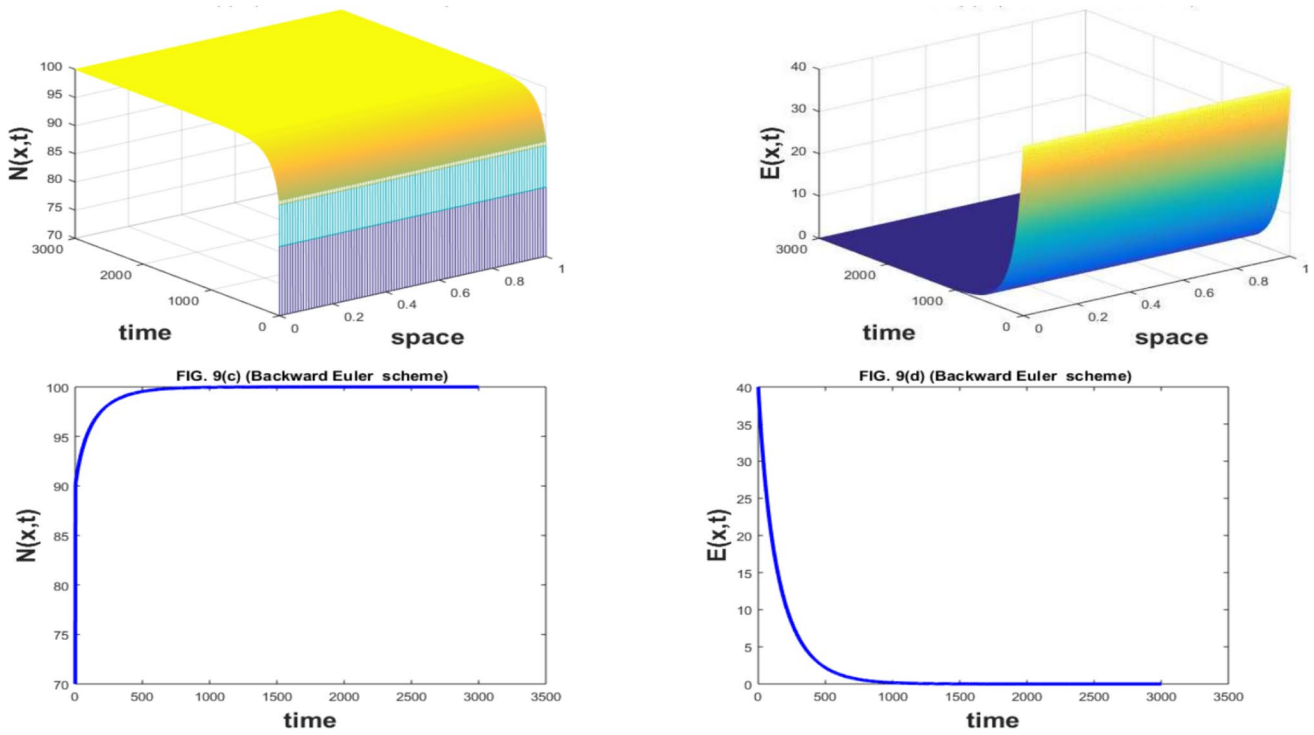

Fig. 9 The 3D and 2D diagrams of fish population and its harvesting by BE scheme for $M = 10, K = 100, c = 0.08$

Fig. 10 The 3D and 2D diagrams of fish population and its harvesting by IFD scheme for $M = 10, K = 100, c = 0.08$

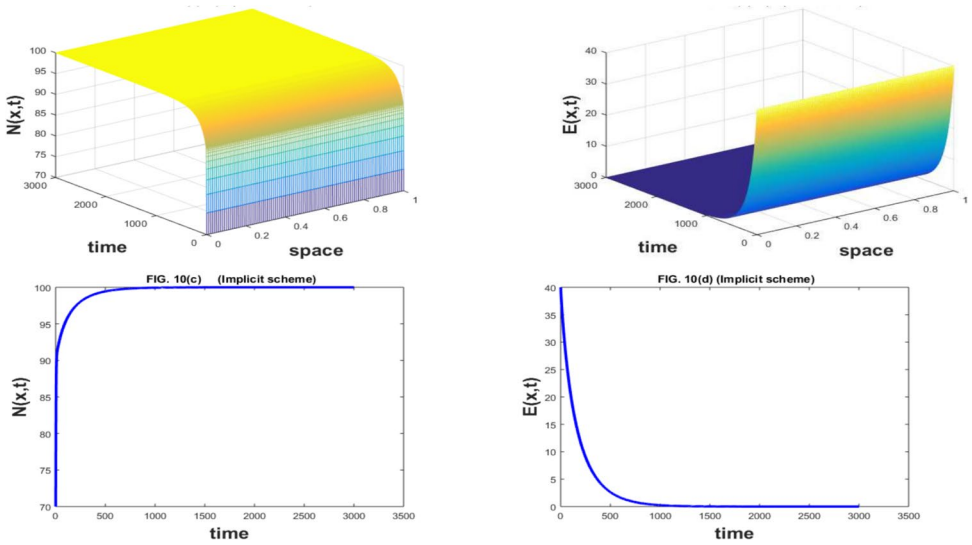

Author contributions All authors have equal contributions.

Data availability No datasets were generated or analysed during the current study.

Declarations

Conflict of interest The authors declare no competing interests.

References

Ahmed N, Jawaz M, Rafiq M, Rehman MA, Ali M, Ahmad MO (2018) Numerical treatment of an epidemic model with spatial diffusion. J Appl Environ Biol Sci 8(6):17–29

Ahmed N, Korkamaz A, Rehman MA, Rafiq M, Ali M, Ahmad MO (2021) Computational modelling and bifurcation analysis of reaction diffusion epidemic system with modified nonlinear incidence rate. Int J Comput Math 98(3):517–535

Ahmed N, Yasin MW, Iqbal MS, Raza A, Rafiq M, Inc M (2023a) A dynamical study on stochastic reaction diffusion epidemic model with nonlinear incidence rate. Eur Phys J Plus 138(4):1–17

Ahmed N, Yasin MW, Ali SM, Akgul A, Raza A, Rafiq M, Shar MA (2023b) Computational aspects of an epidemic model involving stochastic partial differential equations. Int J Mod Phys C

Alfred D (2016) Fish Harvesting Models And Their Applications in a reservoir in Saranda, Albania. J Multidiscip Eng Sci Technol 3(7):5279–5282

Ali KK, AlQahtani SA, Mehanna MS, Wazwaz AM (2023) Novel soliton solutions for the (3+ 1)-dimensional Sakovich equation using different analytical methods. J Math 2023

Bashier EB (2023) A fish harvesting model with Allee effect and Holling type II functional response

Brites NM, Braumann CA (2020) Stochastic differential equations harvesting policies: Allee effects, logistic-like growth and profit optimization. Appl Stoch Model Bus Ind 36(5):825–835

Cooke KL, Nusse HE (1987) Analysis of the complicated dynamics of some harvesting models. J Math Biol 25(5):521–542

Cushing JM, Saleem M (1982) A predator prey model with age structure. J Math Biol 14(2):231–250

Daci A, Spaho A (2013) Bifurcation in a dynamical system: harvest models. In: International conference on research and engineering-challenges toward the future, Albania, pp 24–25

Diz-Pita É, Otero-Espinar MV (2021) Predator-prey models: a review of some recent advances. Mathematics 9(15):1783

Dunn RP, Hovel KA (2020) Predator type influences the frequency of functional responses to prey in marine habitats. Biol Lett 16(1):20190758

Fujimoto T, Ranade R (2004) Two characterizations of inverse-positive matrices: the Hawkins–Simon condition and the Le Chatelier–Braun principle. Electron J Linear Algebra 11:59–65

González-Olivares E, Rojas-Palma A (2011) Multiple limit cycles in a Gause type predator-prey model with Holling type III functional response and Allee effect on prey. Bull Math Biol 73:1378–1397

González-Olivares E, Rojas-Palma A (2013) Allee effect in Gause type predator-prey models: existence of multiple attractors, limit cycles and separatrix curves. A brief review. Math Model Nat Phenom 8(6):143–164

González-Olivares E, Mena-Lorca J, Rojas-Palma A, Flores JD (2011) Dynamical complexities in the Leslie–Gower predator-prey model as consequences of the Allee effect on prey. Appl Math Model 35(1):366–381

González-Olivares E, Cabrera-Villegas J, Córdova-Lepe F, Rojas-Palma A (2019) Competition among predators and Allee effect on prey, their influence on a gause-type predation model. Math Probl Eng 2019

Guo Y, Wang P, Gui W, Yang C (2015) Set stability and set stabilization of Boolean control networks based on invariant subsets. Automatica 61:106–112

Guo Y, Wu Y, Gui W (2021) Stability of discrete-time systems under restricted switching via logic dynamical generator and STP-based mergence of hybrid states. IEEE Trans Autom Control 67(7):3472–3483

Gupta V, Kadalbajoo MK (2016) Qualitative analysis and numerical solution of Burgers' equation via B-spline collocation with implicit Euler method on piecewise uniform mesh. J Numer Math 24(2):73–94

Gupta V, Sahoo SK, Dubey RK (2021) Robust higher order finite difference scheme for singularly perturbed turning point problem with two outflow boundary layers. Comput Appl Math 40:1–23

Huang L, Cai D, Liu W (2020) Optimal harvesting of an abstract population model with interval biological parameters. Adv Differ Equ 2020:1–17

Idels LV, Wang M (2008) Harvesting fisheries management strategies with modified effort function. Int J Model Identif Control 3(1):83–87

Iqbal MS (2011) Solutions of boundary value problems for nonlinear partial differential equations by fixed point methods

Iqbal MS, Ahmed N, Akgül A, Raza A, Shahzad M, Iqbal Z, Jarad F (2022) Analysis of the fractional diarrhea model with Mittag–Leffler kernel. AIMS Math 7:13000–13018

Lv Z, Zhao Q, Li S, Wu Y (2022) Finite-time control design for a quadrotor transporting a slung load. Control Eng Pract 122:105082

Perälä T, Kuparinen A (2017) Detection of Allee effects in marine fishes: analytical biases generated by data availability and model selection. Proc R Soc B Biol Sci 284(1861):20171284

Rojas-Palma A, González-Olivares E (2012) Optimal harvesting in a predator-prey model with Allee effect and sigmoid functional response. Appl Math Model 36(5):1864–1874

Saber S, Bashier E, Alzahrani S, Noaman I (2018) A mathematical model of glucose-insulin interaction with time delay. J Appl Comput Math 7(416):2

Sahoo SK, Gupta V (2022) Higher order robust numerical computation for singularly perturbed problem involving discontinuous convective and source term. Math Methods Appl Sci 45(8):4876–4898

Sahoo SK, Gupta V (2023) A robust uniformly convergent finite difference scheme for the time-fractional singularly perturbed convection-diffusion problem. Comput Math Appl 137:126–146

Seadawy AR, Younis M, Baber MZ, Iqbal MS, Rizvi ST (2022) Nonlinear acoustic wave structures to the Zabolotskaya–Khokholov dynamical model. J Geom Phys 175:104474

Selvam AGM, Janagaraj R, Vignesh D (2018) Allee effect and Holling type-II response in a discrete fractional order prey-predator model. J Phys Conf Ser 1139(1):012003

Shahzad M, Ahmed N, Iqbal MS, Inc M, Baber MZ, Anjum R, Shahid N (2023) Application of fixed point theory and solitary wave solutions for the time-fractional nonlinear unsteady convection-diffusion system. Int J Theor Phys 62(12):263

Shahzad M, Ahmed N, Iqbal MS, Inc M, Baber MZ, Anjum R (2024) Classical regularity and wave structures of fractional order Selkov–Schnakenberg system. Int J Theor Phys 63(4):95

Shi X, Ishtiaq U, Din M, Akram M (2024) Fractals of interpolative Kannan mappings. Fractal Fract 8(8):493

Tesfay A, Tesfay D, Brannan J, Duan J (2021) A logistic-harvest model with Allee effect under multiplicative noise. Stoch Dyn 21(03):2150044

Wu Y, Le S, Zhang K, Sun XM (2021) Agent transformation of Bayesian games. IEEE Trans Autom Control 67(11):5793–5808

Younas U, Ren J, Baber MZ, Yasin MW, Shahzad T (2022) Ion-acoustic wave structures in the fluid ions modeled by higher dimensional generalized Korteweg–de Vries–Zakharov–Kuznetsov equation. J Ocean Eng Sci

Younis M, Seadawy AR, Baber MZ, Yasin MW, Rizvi ST, Iqbal MS (2021) Abundant solitary wave structures of the higher dimensional Sakovich dynamical model. Math Methods Appl Sci